EXACT FEEDBACK LINEARIZATION CONTROL OF A BIDIRECTIONAL DC-DC CONVERTER FOR LI-ION BATTERY/SUPERCAPACITOR HYBRID ENERGY STORAGE SYSTEMS IN ELECTRIC VEHICLES

Bui Van Huy[1,*], Quach Duc Cuong[1], Nguyen Van Doai[1], Bui Thi Thu Ha[1], Tran Duc Hiep[1], Nguyen Son Tung[2]

DOI: https://doi.org/10.57001/huih5804.2026.107

ABSTRACT

Growing concern over pollution from fossil-fuel-based transportation has accelerated the development of electric vehicles (EVs). In EV hybrid energy storage systems (HESS), bidirectional DC-DC converters are key interfaces that coordinate energy exchange between the DC bus and storage devices such as Li-ion batteries and supercapacitors. This study develops an exact feedback linearization controller for a bidirectional DC-DC converter in a Li-ion battery/supercapacitor HESS for EV applications. The exact feedback linearization controller is derived for Boost-mode discharging operation, while Buck-mode charging is implemented using a nominal duty-ratio relation. MATLAB/Simulink simulations are conducted for Buck operation, Boost operation, and the transition between charging and discharging modes. The results indicate that the proposed structure can satisfy the required operating conditions and support stable converter performance in the investigated scenarios.

Keywords: *Li-ion battery, Supercapacitor, Bidirectional DC-DC converter, Exact feedback linearization, Electric vehicle.*

[1]School of Electrical and Electronic Engineering, Hanoi University of Industry, Vietnam

[2]Undergraduate student of Cohort 16, Control and Automation Engineering, Hanoi University of Industry, Vietnam

[*]Email: buivanhuy@haui.edu.vn

Received: 05/3/2026

Revised: 04/5/2026

Accepted: 25/5/2026

1. INTRODUCTION

In recent decades, air pollution caused largely by fossil-fuel-based transportation has become a major threat to public health and sustainable development worldwide [1, 2]. According to the World Health Organization, air pollution contributes to millions of premature deaths each year. In this context, electric vehicles (EVs) are widely regarded as a strategic solution for reducing carbon emissions and promoting sustainable transportation.

Despite the numerous advantages of EVs regarding environmental impact and energy efficiency [3], the energy storage system (ESS) - the core component of EVs - faces several technical challenges. Notably, the optimization of charging and discharging processes remains important for improving dynamic response, power efficiency, and system lifespan, while practical EV applications also require compact and lightweight energy storage hardware [4, 5]. Recent research indicates that combining Li-ion batteries and supercapacitors in an EV energy storage system can improve overall performance by exploiting the complementary characteristics of both technologies [6]. Li-ion batteries, characterized by high energy density (250 - 300Wh/kg) and low self-discharge rates (approximately 3% per month), are widely used in ESSs due to their capacity to deliver stable power over extended periods [7]. However, their limitations in power density (under 1kW/kg) hinder their ability to accommodate sudden load changes [8]. Conversely, supercapacitors, with their exceptionally high power density (10 - 100kW/kg) and a significantly longer cycle life than Li-ion batteries (more than 500,000 cycles), are unsuitable for long-term energy storage. The multi-objective optimization method aims to enhance the performance of hybrid storage systems by allowing

supercapacitors to absorb large current pulses during fluctuations, thereby extending the lifespan of Li-ion batteries and enabling quicker responses to load variations [9]. While Li-ion batteries provide long-term stable power, the output power of the battery pack is constrained to maintain high efficiency and prolong battery life, whereas the supercapacitor output can vary significantly due to its high power density and fast charge-discharge capability. Given the frequent and substantial power fluctuations in electric vehicles, supercapacitors serve as effective energy buffers. The synergistic integration of these two technologies through a bidirectional DC-DC converter has been investigated as a viable solution in [8, 10, 11, 18, 19].

Despite growing interest in hybrid energy storage systems (HESS) for electric vehicles, the application of exact feedback linearization remains limited. Most previous studies have relied on conventional control strategies, which may not provide sufficient accuracy for strongly nonlinear converter dynamics [12, 13]. Exact feedback linearization is particularly attractive for nonlinear systems such as bidirectional DC-DC converters because it transforms the original nonlinear dynamics into an equivalent linear form, thereby enabling more precise voltage and current regulation. Compared with classical PID control, this method can offer higher accuracy and improved dynamic response under varying operating conditions. In addition, unlike sliding-mode control, it can provide smoother behavior while mitigating chattering [14].

Nevertheless, important limitations remain. The performance of exact feedback linearization depends strongly on the accuracy of the system model, which is often difficult to guarantee in practice because of parameter uncertainty, load variation, and external disturbance. In addition, the method generally requires detailed modeling and relatively high computational effort, which may limit its applicability in large-scale or real-time implementations. These considerations help explain why exact feedback linearization, despite its theoretical advantages, has not yet been widely adopted in practical HESS control systems.

The main contribution of this study is the design of an exact feedback linearization controller for a bidirectional DC-DC converter in a Li-ion battery/supercapacitor hybrid energy storage system (HESS) for EVs. Rather than addressing system-level energy management, this study focuses on converter-level control during charging, discharging, and transitions between operating modes. The proposed method aims to achieve three main objectives: (i) maintaining a stable DC-bus voltage, (ii) ensuring appropriate current responses under different operating modes, and (iii) improving the dynamic performance of the converter through a nonlinear control strategy tailored to the converter model.

2. DESIGN AND CONTROL OF A BIDIRECTIONAL DC-DC CONVERTER FOR LI-ION BATTERY/SUPERCAPACITOR HESS IN ELECTRIC VEHICLES

Figure 1 illustrates the energy-exchange structure between the storage devices and the DC bus through bidirectional DC-DC converters. The Li-ion battery and the supercapacitor are connected to the DC bus through separate converters in a fully active configuration. In this study, the converter is the primary control object. Its function is to regulate the switching devices so that energy can be transferred to or from the storage devices during charging and discharging. Within the HESS, the Li-ion battery serves as the main long-term energy source, whereas the supercapacitor compensates for short-term power fluctuations and responds rapidly to transient events.

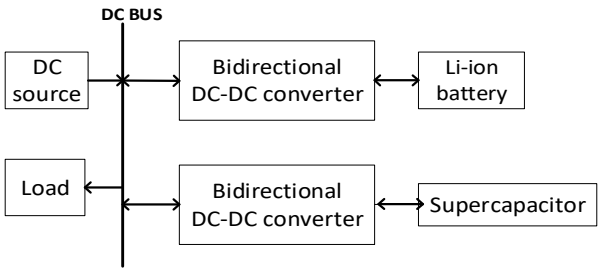

Figure 1. Structure of the Li-ion battery/supercapacitor HESS for EVs

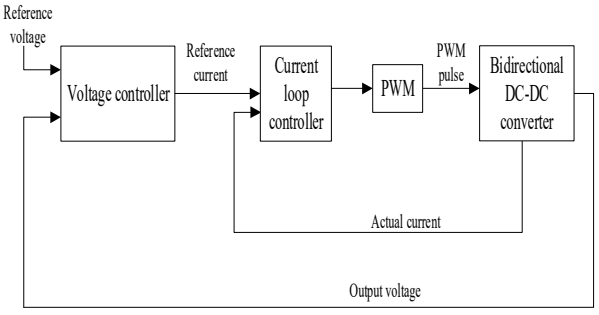

Figure 2. Control-loop structure of the bidirectional DC-DC converter in the HESS

Figure 2 shows the control structure of the bidirectional DC-DC converter. The controller consists of two loops. The outer loop regulates the DC-bus voltage

and generates the reference signal for the inner loop. The inner loop uses the measured inductor current as feedback, compares it with the current reference, and produces the control signal for the PWM modulator. Accordingly, the control objective of this study is converter-level voltage and current regulation for the Li-ion battery/supercapacitor HESS.

2.1. Bidirectional DC-DC converter

Figure 3 illustrates the power-circuit configuration of the bidirectional DC-DC converter. The positive current direction corresponds to the discharging state, whereas the current is negative during charging. The IGBTs are modeled as ideal switches operating at high switching frequency, so the converter is assumed to work in continuous conduction mode (CCM). The control signals of switches S1 and S2 are complementary: when S1 is on, S2 is off, and vice versa. Based on these assumptions, the mathematical models of the converter are derived for both Buck and Boost modes [15].

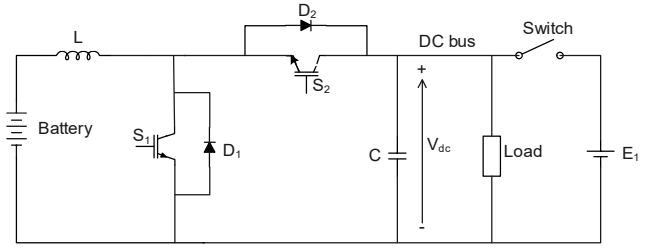

Figure 3. Power circuit of the bidirectional DC-DC converter

2.1.1. Boost mode in discharging HESS

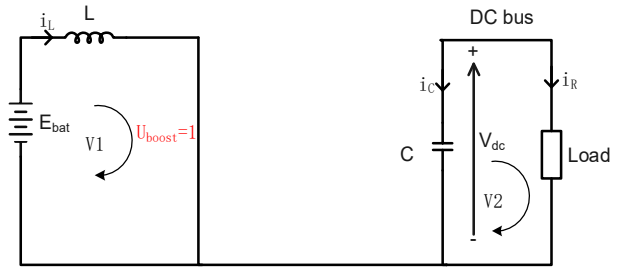

Figure 4. Equivalent circuit of Boost mode when S_1 is on

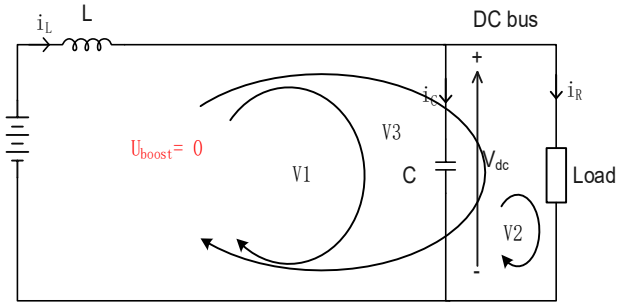

Figure 5. Equivalent circuit of Boost mode when S_1 is off

Figure 4 shows the equivalent circuit of the Boost mode when S1 is on, whereas Figure 5 shows the circuit when S1 is off. Let U_boost denote the control signal of S1, which takes the binary values 0 and 1. Accordingly, U_boost = 1 when S1 is on and U_boost = 0 when S1 is off.

Applying Kirchhoff's laws to the circuit in Figure 4, when S1 is on and diode D2 is off (U_boost = 1), yields:

$$\begin{cases} V_{bat} = L\frac{di_L}{dt} \\ C\frac{dV_{dc}}{dt} = -\frac{V_{dc}}{R} \end{cases} \quad (1)$$

When S1 is off, diode D2 conducts and U_boost = 0. The equivalent Boost-mode circuit is then described by Figure 5. Applying Kirchhoff's laws gives:

$$\begin{cases} L\frac{di_L}{dt} = V_{bat} - V_{dc} \\ C\frac{dV_{dc}}{dt} = i_L - \frac{V_{dc}}{R} \end{cases} \quad (2)$$

Let u_1 denote the duty ratio of IGBT S1, defined as the ratio of its conduction time t1 to the switching period T. Replacing U_boost with u1, the general state equation of the Boost mode can be written as:

$$\begin{cases} L\frac{di_L}{dt} = V_{bat} - (1-u_1)V_{dc} \\ C\frac{dV_{dc}}{dt} = (1-u_1)i_L - \frac{V_{dc}}{R} \end{cases} \quad (3)$$

Equation (3) is normalized by introducing the state variables and scaling factors, where E_max and I_max denote the maximum operating voltage and current, respectively. The normalized form of (3) is then given by:

$$\begin{cases} \dot{x}_1 = a_{11}E_N - a_{12}x_2u \\ \dot{x}_2 = -a_{21}x_2 + a_{22}x_1u \\ y = x_2 \end{cases} \quad (4)$$

where the coefficients in (4) are defined as:

$$\begin{cases} a_{11} = a_{12} = \frac{E_{\max}}{I_{\max}}\sqrt{\frac{C}{L}} \\ a_{21} = \frac{1}{R}\sqrt{\frac{L}{C}} \\ a_{22} = \frac{I_{\max}}{E_{\max}}\sqrt{\frac{L}{C}} = \frac{1}{a_{11}} \end{cases} \quad (5)$$

From the coefficient definitions, it should be noted that $a_{11} = a_{12}$ and $a_{11}a_{22} = 1$. These relations are used to simplify the Lie-derivative expressions in the feedback linearization design.

2.1.2. Buck mode in charging HESS

Let $u_2 = \frac{t_2}{T}$ denote the duty ratio of IGBT S_2, which is defined as the ratio of its active time t_2 within one cycle T; U_{buck} represents the control signal for S2.

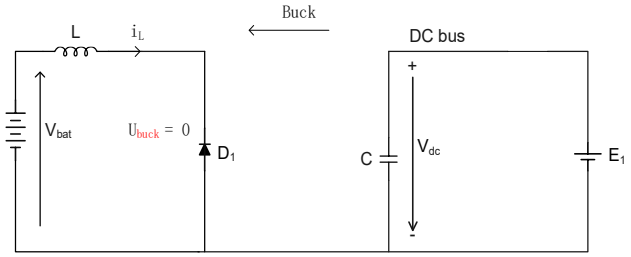

Figure 6. Equivalent circuit of Buck mode when S2 is off

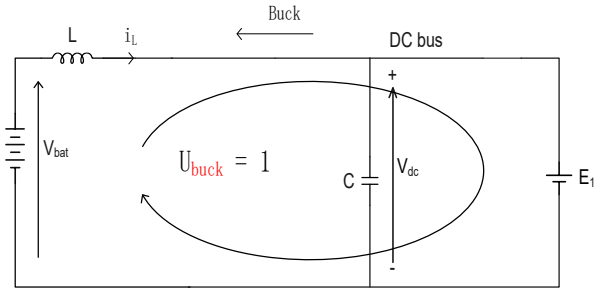

Figure 7. Equivalent circuit of Buck mode when S2 is on

When S_2 is off in Figure 6, diode D_1 conducts and $U_{buck} = 0$. Applying Kirchhoff's laws yields:

$$L\frac{di_L}{dt} = -V_{bat} \quad (6)$$

When S_2 is on in Figure 7, diode D_1 is off and $U_{buck} = 1$. Applying Kirchhoff's laws yields:

$$L\frac{di_L}{dt} = V_{dc} - V_{bat} \quad (7)$$

Replacing U_buck with u_2 and considering the DC-bus voltage as the charging source for the HESS (V_dc = E), the general state equation of the Buck mode is obtained as:

$$\begin{cases} \frac{di_L}{dt} = \frac{1}{L}(u_2 V_{dc} - V_{bat}) \\ V_{dc} = E \end{cases} \quad (8)$$

2.2. Design of an exact feedback linearization controller for the bidirectional DC-DC converter

In this study, the exact feedback linearization controller is developed for the Boost-mode model of the bidirectional DC-DC converter, where the converter exhibits nonlinear dynamics with two state variables. Buck-mode operation is considered as a current-regulated charging process, in which the duty ratio is determined from the charging-current requirement and the ideal Buck conversion relation. Therefore, the main objective of this section is to derive the Boost-mode feedback linearization controller and to define the corresponding Buck-mode duty-ratio relation used during charging.

Based on (4), the rank condition required for input-state exact feedback linearization is examined as follows [16, 17]:

$$C = [h(x) \quad ad_f h(x)] = \begin{bmatrix} -a_{11}x_2 & a_{11}a_{21}x_2 \\ a_{22}x_1 & E_N + a_{22}a_{21}x_1 \end{bmatrix},$$
$$\det(C) = -x_2(a_{11}E_N + 2a_{21}x_1) \neq 0 \quad (9)$$

The rank of matrix C is equal to 2, which matches the system order. Therefore, the rank condition for local accessibility is satisfied. Next, the relative degree associated with the original output $y = x_2$ is examined.

$$L_h x_2 = \frac{\partial x_2}{\partial x} h(x) = [0 \quad 1]\begin{bmatrix} -a_{11}x_2 \\ a_{22}x_1 \end{bmatrix} = a_{22}x_1 \neq 0 \quad (10)$$

According to (10), the original output $y = x_2$ has relative degree (r =1), which is lower than the system order. Therefore, the virtual output $y' = \lambda(x)$ is introduced for input-state exact feedback linearization. The nonlinear model in (4) is now expressed as (11):

$$\begin{cases} \frac{d\underline{x}}{dt} = \underline{f}(\underline{x}) + \underline{h}(\underline{x})u \\ y' = \lambda(\underline{x}) \end{cases} \quad (11)$$

From (11), the conditions for applying input-state exact feedback linearization are verified by examining the involutivity of the distribution spanned by $h(x)$.

$$\Delta(x) = \text{span}\{h(x)\};$$
$$[h, h] = \frac{\partial h}{\partial x}h - \frac{\partial h}{\partial x}h = 0 \in \Delta(x) \quad (12)$$

From (12), the distribution spanned by $h(x)$ is involutive; therefore, the nonlinear system can be controlled by the input-state exact feedback linearization method. The scalar function corresponding to the virtual output is then determined as:

$$L_{\underline{h}}\lambda(\underline{x}) = \frac{\partial \lambda(\underline{x})}{\partial \underline{x}}\underline{h}(\underline{x}) = 0$$
$$\Rightarrow \lambda(\underline{x}) = \frac{1}{2}[a_{22}x_1^2 + a_{12}x_2^2] \quad (13)$$

After obtaining the scalar function, the Lie derivatives are calculated as follows:

$$L_{\underline{f}}\lambda(\underline{x}) = x_1 E_N - a_{11}a_{21}x_2^2$$
$$L_{\underline{f}}^2\lambda(\underline{x}) = a_{11}(E_N^2 + 2a_{21}^2x_2^2) \quad (14)$$
$$L_{\underline{h}}L_{\underline{f}}\lambda(\underline{x}) = -a_{11}x_2E_N - 2a_{21}x_1x_2$$

From the Lie derivatives above, the exact feedback controller, the state-coordinate transformation, and the corresponding linearized model can be derived. However, the linearized model is not asymptotically stable because it contains repeated poles at s = 0. The nonlinear system is therefore stabilized using an exact feedback linearization controller with preassigned poles s_1 and s_2, yielding:

$$w = \ddot{\tilde{y}} = -a_1\dot{\tilde{y}} - a_0(\tilde{y} - Y)$$
$$= -a_1 z_2 - a_0(z_1 - Y) \quad (15)$$

where a_0, a_1, z_1, z_2, and Y are determined by:

$$(s - s_1)(s - s_2) = s^2 + a_1 s + a_0; z_2 = L_f\lambda(\underline{x})$$

$$z_1 = \lambda(\underline{x}) = \frac{1}{2}[a_{22}x_1^2 + a_{11}x_2^2];$$

$$Y = \frac{1}{2}[a_{22}\bar{x}_1^2 + a_{11}\bar{x}_2^2]$$

Here, x denotes the state vector, u is the input variable, and Y denotes the reference value in the transformed coordinate, corresponding to the desired DC-bus voltage operating point. Substituting z_1, z_2, and Y into (15), the input variable w is obtained as:

$$w = -a_1(x_1 E_N - a_{11}a_{21}x_2^2)$$
$$-\frac{a_0}{2}\left[a_{22}x_1^2 + a_{11}x_2^2 - a_{22}\left(\frac{a_{11}a_{21}V_d^2}{E_N}\right)^2 - a_{11}V_d^2\right] \quad (16)$$

where V_d denotes the desired value of the normalized DC-bus voltage.

The exact feedback linearization controller with preassigned poles is given by:

$$u = \frac{a_{11}(E_N^2 + 2a_{21}^2x_2^2) - w}{a_{11}E_N x_2 + 2a_{21}x_1x_2} \quad (17)$$

The state-coordinate transformation is given by:

$$\underline{z} = \begin{bmatrix} z_1 \\ z_2 \end{bmatrix} = \begin{pmatrix} \lambda(\underline{x}) \\ L_f\lambda(\underline{x}) \end{pmatrix} = \begin{pmatrix} \frac{1}{2}[a_{22}x_1^2 + a_{12}x_2^2] \\ x_1E_N - a_{11}a_{21}x_2^2 \end{pmatrix} \quad (18)$$

The resulting linearized model is:

$$\begin{cases} \dot{z}_1 = z_2 \\ \dot{z}_2 = -a_0(z_1 - Y) - a_1 z_2 \end{cases} \quad (19)$$

Based on the general state equation, an ideal steady-state duty-ratio relation for Buck-mode operation can be obtained as (20).

$$u_n = \frac{V_{bat}}{V_{dc}} \quad (20)$$

This relation provides a nominal duty-ratio value for Buck-mode charging operation under ideal steady-state conditions.

3. RESULTS AND DISCUSSION

Based on the mathematical model and the proposed controller, a MATLAB/Simulink model of the bidirectional DC-DC converter for the Li-ion battery/supercapacitor HESS is developed. The simulations focus on converter-level behavior in three operating scenarios: Buck mode during charging, Boost mode during discharging, and the transition between charging and discharging.

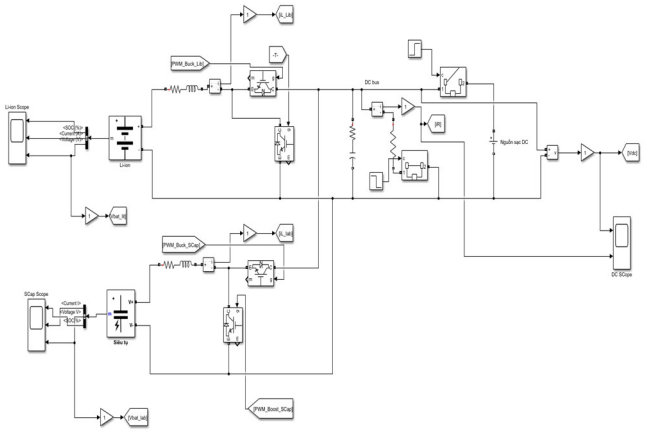

Figure 8. The model of power circuit in MATLAB/Simulink

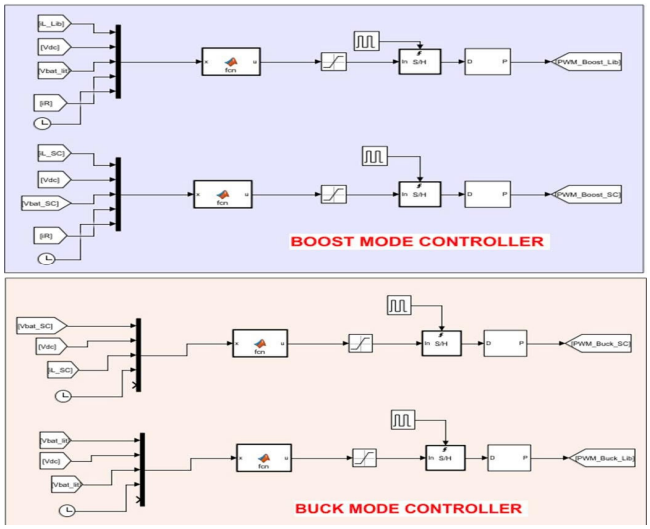

Figure 9. The model of control loop circuit in MATLAB/Simulink

The main simulation parameters include a switching frequency of 5kHz, a DC-bus voltage reference of 300V, and preassigned poles at s_1 = -1 and s_2 = -2. These poles are selected to ensure closed-loop stability while maintaining a moderate response speed and avoiding excessive overshoot or control effort. A switching frequency of 5kHz provides a practical trade-off between ripple reduction and switching loss.

The Li-ion battery and supercapacitor parameters used in the converter simulation are presented in Tables 1 and 2.

Table 1. Parameters of the Li-ion battery

No.	Parameter	Value
1	Nominal voltage (V)	150
2	Rated capacity (Ah)	50
3	Initial state-of-charge (%)	50
4	Battery response time (s)	30

Table 2. Parameters of the supercapacitor

No.	Parameter	Value
1	Rated capacitance (F)	8
2	Equivalent DC series resistance (Ohms)	8.9×10^{-3}
3	Rated voltage (V)	150
4	Number of series capacitors	15
5	Number of parallel capacitors	1
6	Initial voltage (V)	118.6
7	Operating temperature (°C)	25

3.1. Case 1: Buck mode when charging the HESS

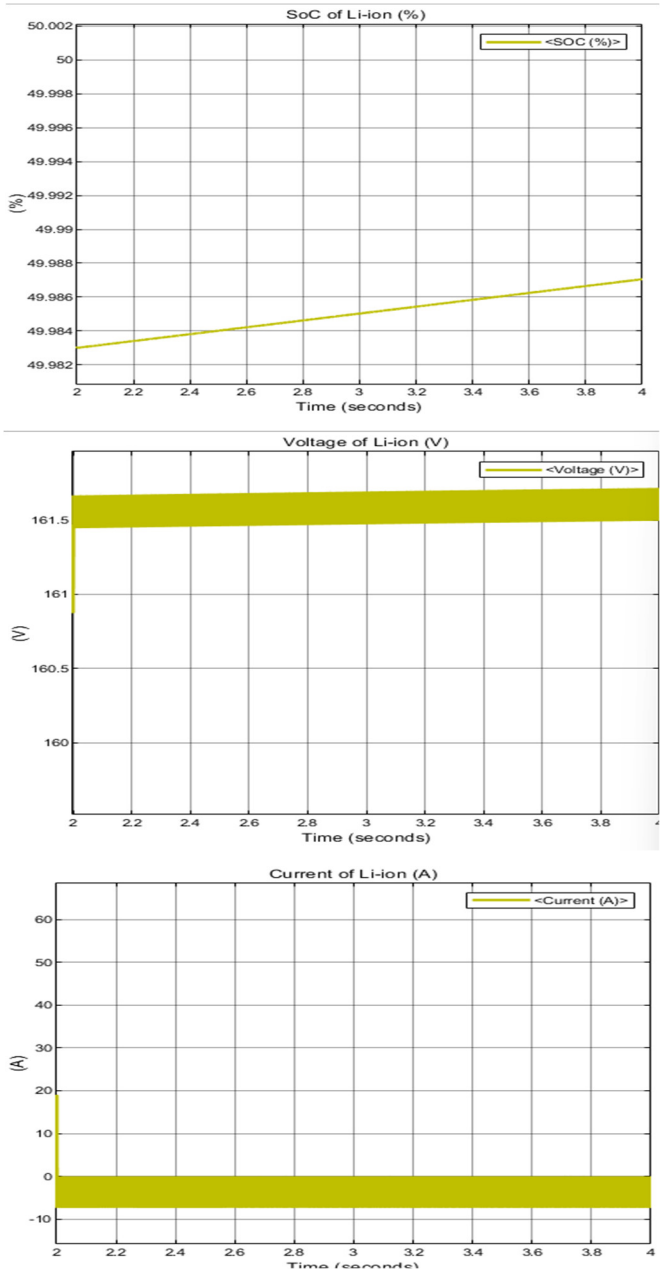

Figure 10. Simulation results of Li-ion battery in case 1

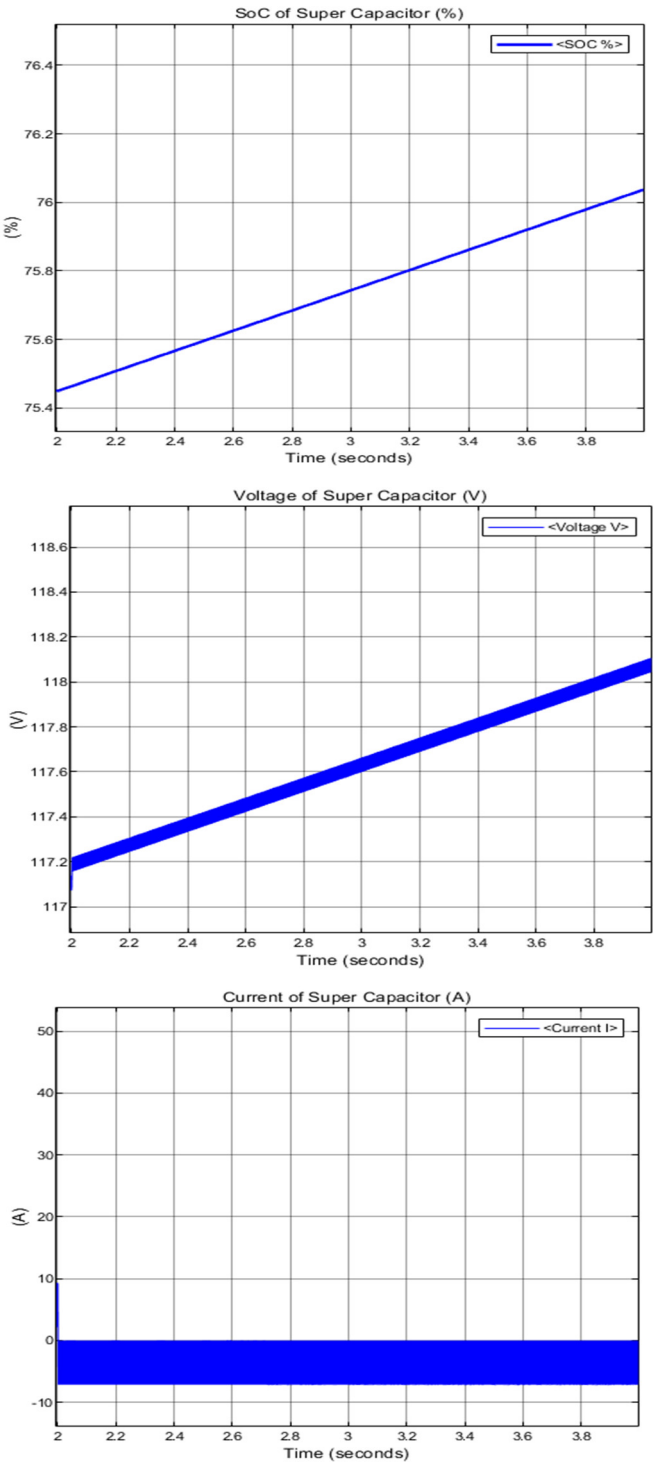

Figure 11. Simulation results of supercapacitor in case 1

The Buck-mode simulation results describe the converter behavior during HESS charging. Figures 10 and 11 illustrate the dynamic response of the Li-ion battery and supercapacitor under converter-controlled charging conditions. The trends of voltage, state of charge, and charging current indicate that the storage devices absorb energy through the bidirectional DC-DC converter under the simulated Buck-mode condition.

During charging, the storage-device voltages increase slightly while remaining well regulated. The Li-ion battery voltage increases slightly from approximately 161V to 161.55V, whereas the supercapacitor voltage increases from 117.2V to 118.1V. The negative charging current is consistent with the defined charging direction, indicating that energy flows into the storage devices.

Overall, the Buck-mode results show that the proposed control structure can maintain a stable charging current and support reliable energy storage without abrupt electrical variations. This behavior is important for safe converter operation and for limiting excessive stress on the storage devices.

3.2. Case 2: Boost mode when discharging the HESS

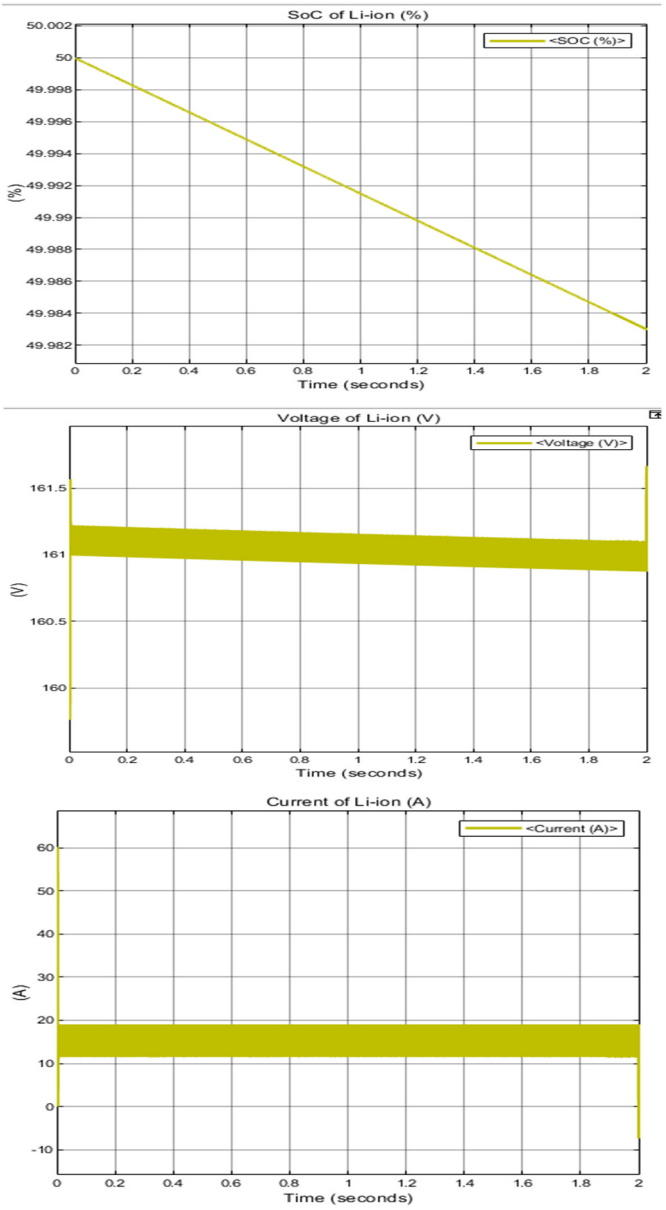

Figure 12. Simulation results of Li-ion battery in case 2

The simulation results for Boost mode during HESS discharging, shown in Figures 12, 13, and 14, highlight the converter performance in regulating voltage, current, and energy transfer from the storage devices to the DC bus.

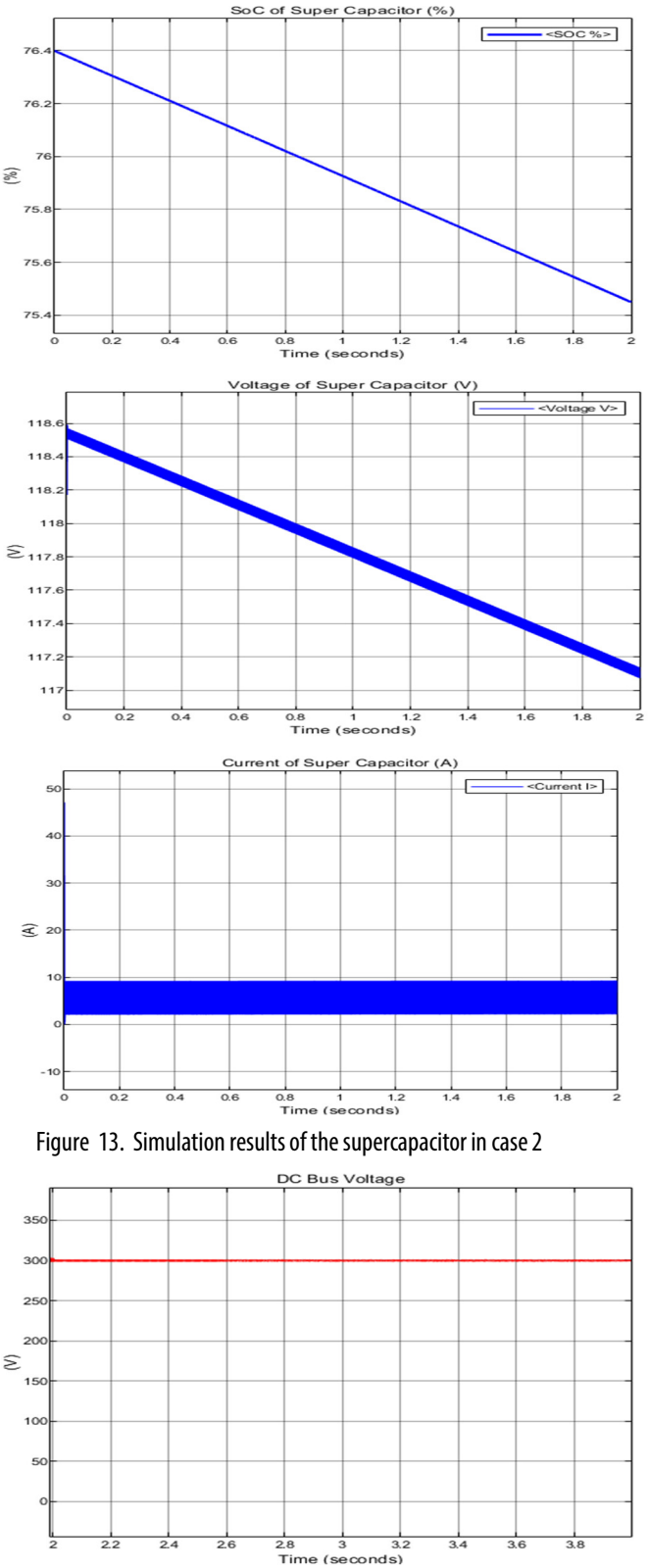

Figure 13. Simulation results of the supercapacitor in case 2

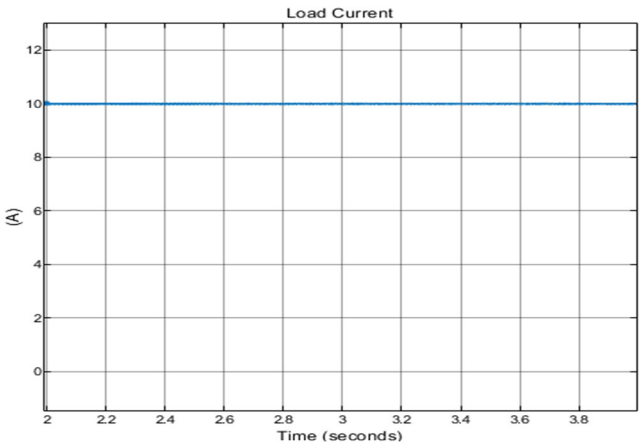

Figure 14. DC-bus voltage and load current in case 2

The DC-bus voltage remains close to the 300V reference, indicating that the bidirectional DC-DC converter is able to regulate the DC-bus voltage under the simulated Boost-mode condition. During discharge, the battery and supercapacitor voltages show a decreasing tendency as energy is supplied from the HESS to the load. The storage-device currents remains positive with limited fluctuation, which is consistent with the expected power-flow direction from the HESS to the DC bus. These results indicate that the proposed exact feedback linearization method can provide a stable and well-damped converter response in Boost mode.

Overall, the Boost-mode results suggest that the converter can manage the discharging operation, maintain the DC-bus voltage near its reference value, and support relatively consistent current flow under the considered simulation conditions.

3.3. Case 3: Transition between discharging and charging modes

The third scenario evaluates converter behavior during the transition between discharging and charging, as shown in Figures 15, 16, and 17.

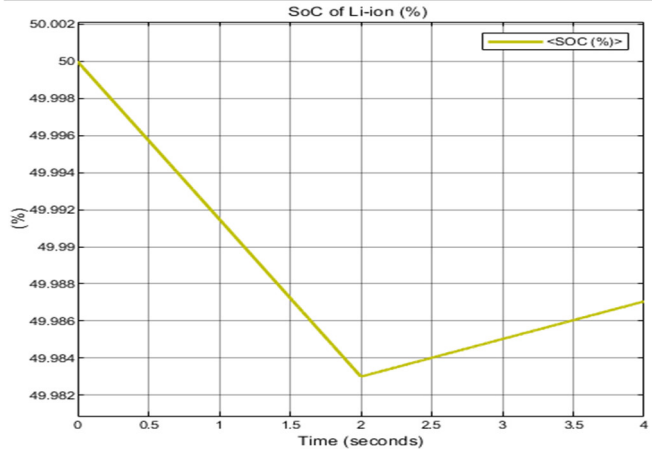

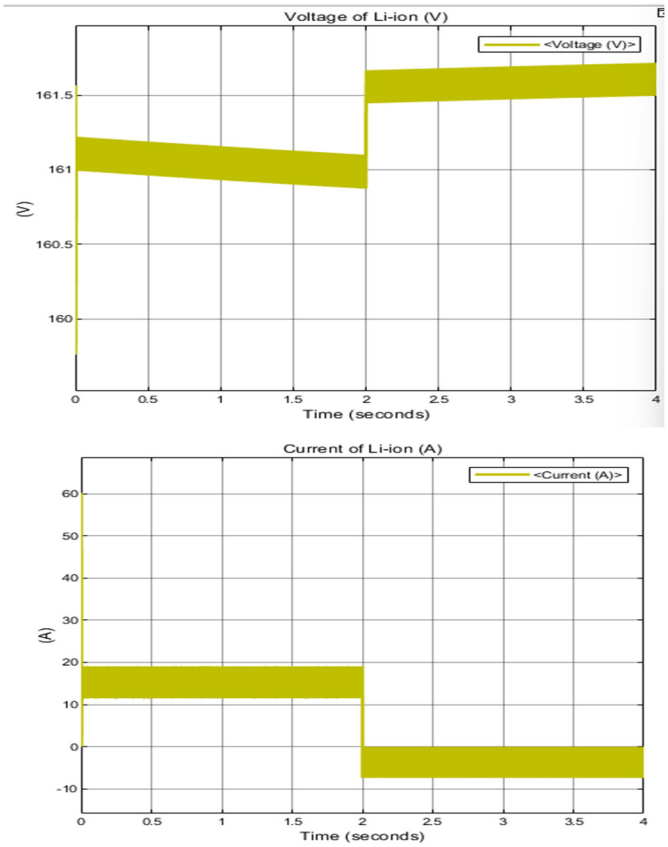

Figure 15. Simulation results of Li-ion battery in case 3

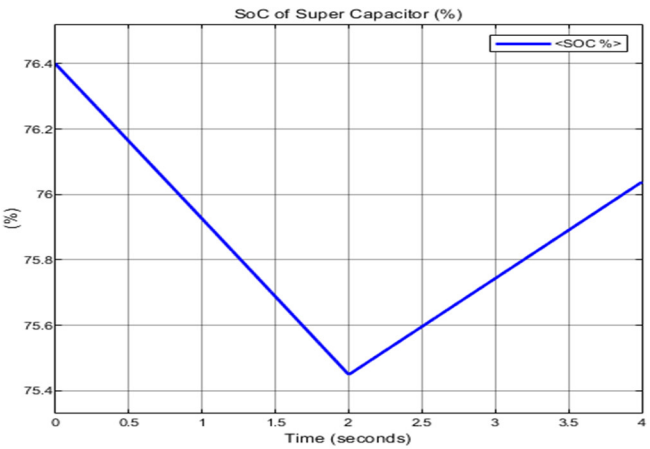

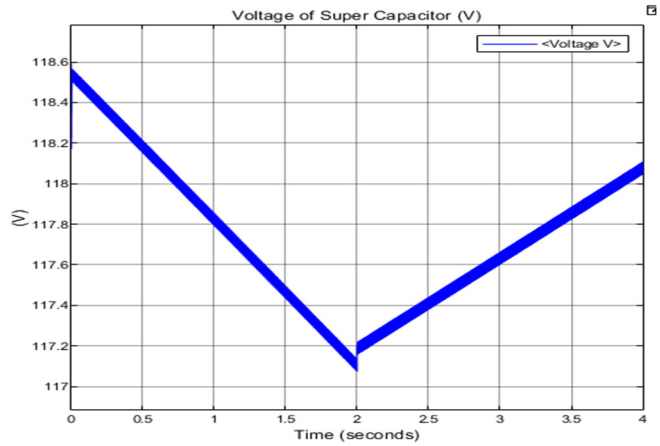

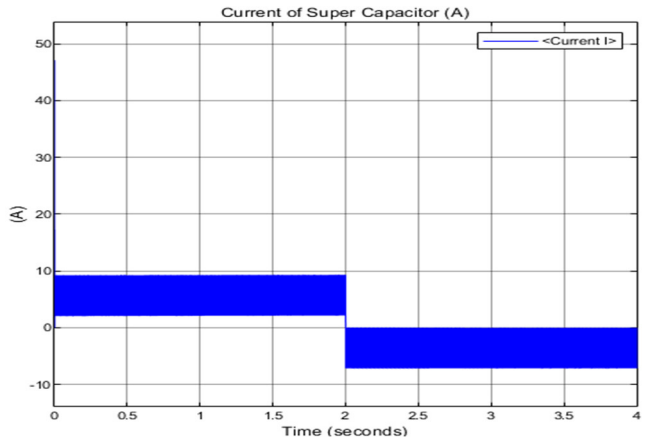

Figure 16. Simulation results of the supercapacitor in case 3

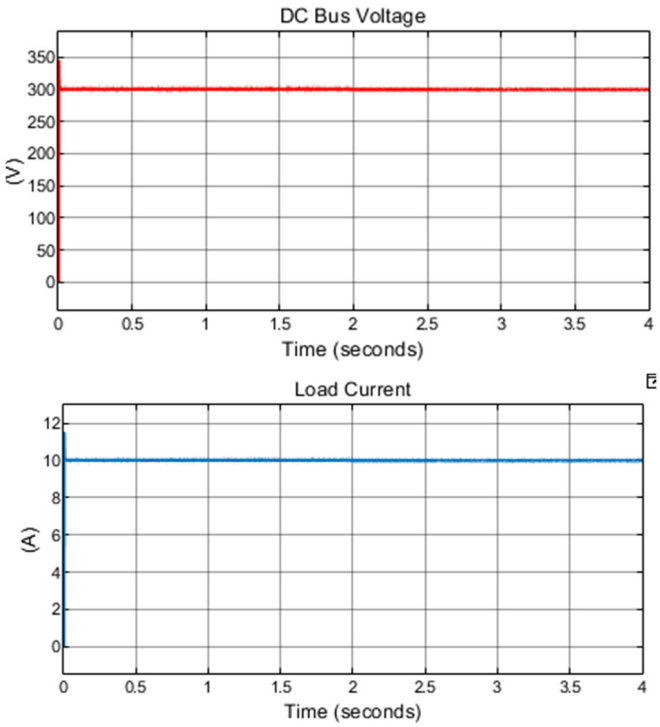

Figure 17. DC-bus voltage and load current in case 3

The simulation results show that the battery and supercapacitor voltages, together with their state-of-charge values, decrease during the initial discharging interval as the HESS supplies energy to the load. After the transition instant, these quantities begin to increase, indicating that the converter changes to charging operation. This behavior is consistent with the intended transition from Boost mode to Buck mode and suggests a stable change in the power-flow direction.

During the discharging interval, the battery and supercapacitor currents are positive, which is consistent with the selected reference direction for power delivery from the HESS to the DC bus. After the system changes to charging mode, the currents become negative, indicating reverse power flow and Buck-mode charging operation. Although a current step occurs at the transition instant, the currents remain bounded and settle to the expected levels. The DC-bus voltage remains close to 300V throughout the transition, showing that the converter can pass through the mode change without a noticeable DC-bus voltage deviation under the simulated conditions.

4. CONCLUSION

This paper has presented a control method for a bidirectional DC-DC converter in a Li-ion battery/supercapacitor hybrid energy storage system for electric vehicles. The study focuses on converter-level control rather than on a complete energy-management strategy for the entire HESS. Simulation results under Buck mode, Boost mode, and mode-transition conditions show that the proposed structure can regulate the DC-bus voltage, maintain an appropriate current response, and support stable converter behavior under the investigated operating conditions.

The work is currently limited to simulation, and the converter model is still based on idealized assumptions that neglect practical effects such as sensor noise, switching delays, parasitic elements, and controller implementation constraints. Future research should therefore include hardware validation, robustness assessment under parameter uncertainty, and integration of the converter controller into a higher-level energy management system for electric vehicles.

REFERENCES

[1]. K. V. Singh, H. O. Bansal, D. Singh, "A comprehensive review on hybrid electric vehicles: architectures and components," *Journal of Modern Transportation*, 27, 2, 77-107, 2019, doi: 10.1007/s40534-019-0184-3.

[2]. A. A. El Baset A. El Halim, E. Bayoumi, W. El-Khattam, A. Ibrahim, "Electric vehicles: a review of their components and technologies," *International Journal of Power Electronics and Drive Systems*, 13, 2041-2061, 2022. doi: 10.11591/ijpeds.v13.i4.pp2041-2061.

[3]. T. Christen, M. W. Carlen, "Theory of Ragone plots," *J Power Sources*, 91, 2, 210–216, 2000. doi: 10.1016/S0378-7753(00)00474-2.

[4]. N. D. Quang, "Research and review on battery for electric vehicles: Technology, models and calculating simulation for battery performance in GM EV1," *Journal of Science and Technology of Energy - Electric Power University*, 31, 1-11, 2023.

[5]. L. Guo, D. Thornton, M. Koronfel, I. Stephens, M. Ryan, "Degradation in lithium ion battery current collectors," *Journal of Physics: Energy*, 3, 2021. doi: 10.1088/2515-7655/ac0c04.

[6]. A. Khaligh, Z. Li, "Battery, Ultracapacitor, Fuel Cell, and Hybrid Energy Storage Systems for Electric, Hybrid Electric, Fuel Cell, and Plug-In Hybrid Electric Vehicles: State of the Art," *IEEE Trans Veh Technol*, 59, 6, 2806-2814, 2010. doi: 10.1109/TVT.2010.2047877.

[7]. K. Dissanayake, D. Kularatna-Abeywardana, "A review of supercapacitors: Materials, technology, challenges, and renewable energy applications," *J Energy Storage*, 96, p. 112563, 2024. doi: 10.1016/J.EST.2024.112563.

[8]. M. Kurtoğlu, F. Eroğlu, "Design and simulation of bidirectional DC-DC converter topology for battery applications," *E3S Web of Conferences*, 551, p. 03002, 2024. doi: 10.1051/e3sconf/202455103002.

[9]. S. Aragon-Aviles, A. H. Kadam, T. Sidhu, S. S. Williamson, "Modeling, Analysis, Design, and Simulation of a Bidirectional DC-DC Converter with Integrated Snow Removal Functionality for Solar PV Electric Vehicle Charger Applications," *Energies (Basel)*, 15, 8, 2022. doi: 10.3390/en15082961.

[10]. H. Sira-Ramírez, R. Silva-Ortigoza, *Control Design Techniques in Power Electronics Devices*. Springer London, 2006.

[11]. Y. A. Makandar, S.S.Vanamane, "Performance Analysis of Bidirectional DC-DC Converter for Electric Vehicle Application," *International Journal for Innovative Research in Science and Technology*, 1, 43-49, 2015. [Online]. Available: https://api.semanticscholar.org/CorpusID:16752739

[12]. Y. Yin, J. Mao, R. Liu, "Multivariable-Feedback Sliding-Mode Control of Bidirectional DC/DC Converter in DC Microgrid for Improved Stability with Dynamic Constant Power Load," *Electronics*, 11, 3455, 2022. doi: 10.3390/electronics11213455.

[13]. L. Wang, T. Miao, X. Liu, S. Liu, "Sliding Mode Control of Bi-directional DC/DC Converter in DC Microgrid Based on Exact Feedback Linearization," *Wseas Transactions on Circuits and Systems*, 19, 206-211, 2020. doi: 10.37394/23201.2020.19.23.

[14]. D. Palwalia, A. Sharma, "An review: Control strategies in bidirectional DC-DC converter topologies," *International Journal of Technical Research & Science*, 9, 27-35, 2024. doi: 10.30780/specialissue-ISET-2024/030.

[15]. X. Zhao, B. Li, Q. Fu, Y. Zhang, S. Mao, D. Xu, "A Isolated Bidirectional DC/DC Converter with Low-Voltage IGBTs for Solid-State Transformers," in *2020 4th International Conference on HVDC, HVDC 2020*, 982-985, 2020. doi: 10.1109/HVDC50696.2020.9292754.

[16]. N. D. Phuoc, *Nonlinear Systems Control Analysis*. Bach Khoa Publisher, 2012.

[17] Q. Lu, Y. Sun, S. Mei, *Nonlinear Control Systems and Power System Dynamics*. Springer US, 2001. doi: 10.1007/978-1-4757-3312-9/COVER.

[18]. Bui Van Huy, Trinh Trong Chuong, Quach Duc Cuong, "Research and simulation of a hybrid supercapacitor-lithium battery energy storage system for solar energy," *TNU Journal of Science and Technology* 228(14): 214-221, 2023. doi: https://doi.org/10.34238/tnu-jst.8852

[19]. Nguyen Duc Minh, Bui Van Huy, Ngo Thi Quan, Nguyen Quang Ninh, Trinh Trong Chuong, "Research and design of grid-connected inverter in photovoltaic system with SVPWM technique," *International Journal of Engineering Technologies and Management Research,* 6, 11, 2019. doi: https://doi.org/10.29121/ijetmr.v6.i11.2019.4600.